

A sharp multiplier theorem for solvable extensions of Heisenberg and related groups

Original

A sharp multiplier theorem for solvable extensions of Heisenberg and related groups / Martini, Alessio; Plewa, Pawel Mateusz. - In: ANNALI DI MATEMATICA PURA ED APPLICATA. - ISSN 0373-3114. - 203:3(2024), pp. 1361-1408. [10.1007/s10231-023-01405-z]

Availability:

This version is available at: 11583/2984714 since: 2024-06-03T13:12:17Z

Publisher:

Springer

Published

DOI:10.1007/s10231-023-01405-z

Terms of use:

This article is made available under terms and conditions as specified in the corresponding bibliographic description in the repository

Publisher copyright

Springer postprint/Author's Accepted Manuscript

This version of the article has been accepted for publication, after peer review (when applicable) and is subject to Springer Nature's AM terms of use, but is not the Version of Record and does not reflect post-acceptance improvements, or any corrections. The Version of Record is available online at: <http://dx.doi.org/10.1007/s10231-023-01405-z>

(Article begins on next page)

A pilot study on the use of high-frequency photoacoustic imaging for quantitative human skin vasculature analysis

Bruna Cotrufo, Alberto Vallan, Silvia Seoni, Giacinto Luigi Cerone, Alberto Botter,
Filippo Molinari and Kristen M. Meiburger
Department of Electronics and Telecommunications, Politecnico di Torino, Turin, Italy

ABSTRACT

The assessment of skin health often relies on detailed visualization of skin architecture and its underlying vascular structures. A non-invasive technique which allows vasculature imaging is photoacoustic imaging (PAI), a hybrid modality that combines advantages from both optical and ultrasound imaging. This pilot study explores the efficacy of a high-frequency, linear array-based photoacoustic and ultrasound imaging setup for skin vasculature analysis. A PAI setup was developed involving a high-frequency linear probe employing capacitive micromachined ultrasound transducers (CMUT) as detectors with a central frequency of 30 MHz (operating at 22 MHz) and a bandwidth of 60 %. One healthy volunteer was imaged at four different locations and the photoacoustic images were automatically segmented and quantified, providing quantitative parameters of the vascular network complexity. Preliminary results demonstrate the potential of such setup to effectively segment superficial vasculature. Future studies will aim to expand on these findings and incorporate a quantitative analysis comparing with pathological cases, as well as hardware and software improvements to enhance image quality, mitigate artifacts, and optimize the system's usability in clinical settings.

Keywords: photoacoustics, high-frequency linear array, human skin, vasculature analysis

1. INTRODUCTION

Analyzing the complexity of the skin vasculature network is crucial for understanding various physiological and pathological conditions, as it can provide insights into tissue health, perfusion, and the body's response to injury or disease. Dermoscopy and histological examination are currently the gold standards for skin diseases diagnosis. However, these techniques have several drawbacks: dermoscopy is prone to a large number of lesion misclassifications while biopsy followed by histological examination is invasive and requires a long-term procedure from the surgery to the diagnosis [1, 2]. In this context, the possibility to non-invasively image in-vivo skin vasculature led to the translation of optical imaging techniques into dermatology. To address the limited penetration depth of pure optical imaging systems, photoacoustic imaging (PAI) has emerged as a complementary technique that combines the high contrast provided by optical absorption and the deeper tissue penetration and spatial resolution of ultrasound. Short pulses of laser light irradiate a biological tissue where chromophores, such as hemoglobin, absorb part of that energy causing thermoelastic expansion and generating wideband acoustic signals detected by US transducers. Among the diverse applications of PAI, skin imaging has emerged as a particularly important area of focus due to its potential for assessing microvascular networks and pathological changes with high precision [3].

The transducer geometry significantly impacts the quality of PA images. A wide range of transducer configurations have been explored in PAI. However, linear arrays are handheld operable, affordable and compatible with conventional and commercial ultrasound systems for simultaneous acquisition, making them the most widely used transducers [4, 5]. The frequency content of the PA signal is determined by the incident wavelength as well as the shape and size of the targets, leading to wideband signals. Although the penetration depth is typically limited to a few millimeters, operating at frequencies above 20 MHz, high-frequency acoustic waves with shorter wavelengths provide superior spatial resolution [6]. The use of high-frequency linear arrays in PA setups has been shown to play a key role in imaging superficial targets, both on phantoms and in-vivo [7-9]. In this perspective, the fabrication process of capacitive micromachined ultrasonic transducers (CMUT) allows for smaller pitch compared to traditional piezoelectric arrays fabricated by mechanical dicing, resulting in higher frequency transducers, reduced aliasing and greater versatility in array design [10]. Furthermore, a wider fractional bandwidth, better acoustic matching, higher resolution and sensitivity, low costs and easy integration with

electronic circuits have made CMUT a strong alternative to conventional piezoelectric transducers, although further efforts are required to improve performance and durability and demonstrate the capability of CMUT probes also for high frequency applications [11-13].

In this pilot study, a PA system equipped with a high-frequency CMUT linear array transducer was used to explore in vivo imaging of human skin and superficial structures for the first time for the automatic quantification of the vasculature network complexity.

2. METHODS

PA system

The high-frequency transducer involved in this study is a commercial 256-element CMUT linear array (L38-22v, Kolo Medical, San Jose, CA) characterized by a pitch of 0.069 mm and a center frequency of 30 MHz (bandwidth: 60%). The probe was configured to operate at a center frequency of 22 MHz. The light source is a pulsed Nd:YAG laser (Phocus SE Mobile, OPOTEK, LLC, USA) operating at a repetition rate of 20 Hz, with a pulse width of 7 ns and tunable wavelength (690–950 nm). A wavelength of 800 nm and an average pulse energy equal to 25 mJ were used. The laser bundle was divided into two 50 mm fiber slits covered with 3D-printed diffusers to ensure meeting laser safety guidelines, resulting in two rectangular illumination areas of approximately 10 x 50 mm. Each slit was angled at approximately 60° with respect to the probe axis. A 3D-printed holder was designed to precisely align the slits with the probe and integrate them into a single, easily manageable unit. The Verasonics Vantage 256 High Frequency system (Verasonics, USA) was used for the acquisition of US and PA data. Fluctuations in the laser optical build-up time cause PA signal jitter when the internal Q-switch trigger is used [14]. To properly synchronize pulse delivery and image acquisition and minimize PA signal jitter, the laser Q-switch input was set to be externally triggered and a custom trigger circuit, referred to as the “trigger box”, was developed. In this setup, the laser flash lamp output is connected to the Verasonics trigger input, while the Verasonics trigger output is connected to the trigger box that inverts the signal and makes it compatible with the laser Q-switch input. The *flash2Qdelay* parameter in Verasonics scripts was set to 190 μ s, preventing laser damage by limiting the released energy. A schematic of the system is shown in Fig. 1.

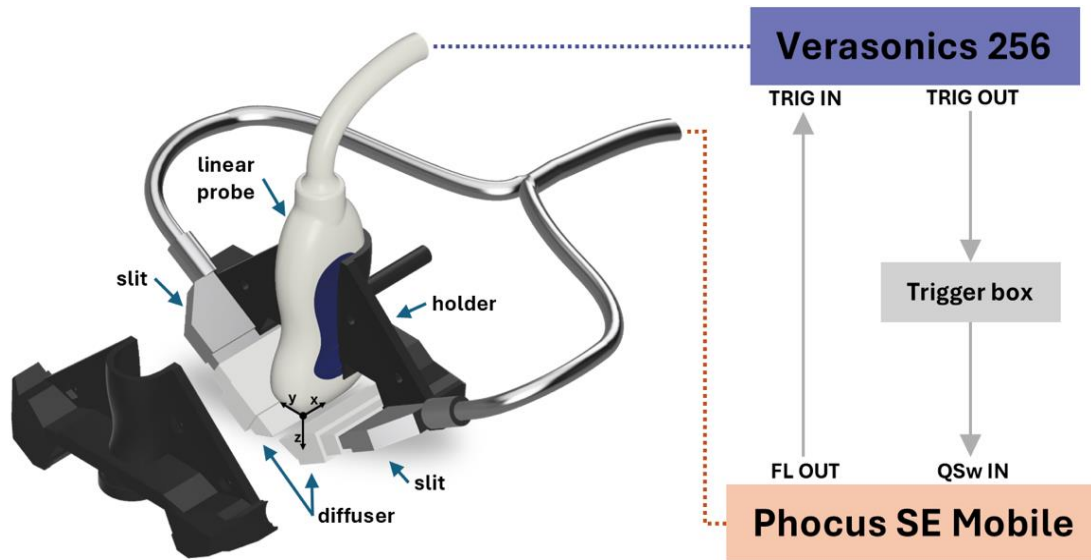


Figure 1. Schematic of the PA system. The laser flash lamp output signal is used to trigger the Verasonics that, with a delay of 190 μ s, triggers the laser Q-switch input after the “trigger box” conditioning.

Experimental protocol and data processing

The probe holder was mounted on a three-axis positioning stage system and 3D in-vivo scans of 1 healthy subject across four different locations (wrist, forearm, hand and leg) were acquired translating the probe holder along the y-axis with steps of 1 mm, covering a total area of about 17.6 x 15 mm. At each location, 30 2D x-z scans were acquired and averaged.

The Vantage 256 was used in the high frequency configuration with the interleaved sampling technique for a single B-scan reconstruction. Briefly, to manage high sampling rate, the effective A/D converter sample rate is doubled by combining samples from two successive transmit-receive acquisitions, with the second acquisition's sampling points shifted by half the A/D sampling period.

In order to automatically segment the photoacoustic image, the averaged frames were contrast adjusted with a contrast limited adaptive histogram equalization technique (Fig. 2A) and then a 3D median filter was employed (Fig. 2B). Then, an adaptive threshold was identified automatically by analyzing the intensity histogram of each single 2D frame [15]. Global thresholding was employed and the entire volume was then processed with a 3D morphological opening process (sphere, 1 pixel radius) and then connected objects smaller than 100 pixels were removed (Fig. 2C). Finally, a medial axis skeletonization technique was employed to extract the skeleton of the segmentation (Fig. 2D).

Then, six quantitative features were extracted by analyzing the skeleton. The number of trees (NT), the number of branches (NB) and the vascular density (VD) were used to evaluate morphology. Tortuosity was assessed through the distance metric (DM), defined as the ratio between the actual vessel length and the linear distance between its endpoints, the inflection count metric (ICM), which represents the number of inflection points along the vessels path multiplied by the DM, and the sum of angles metric (SOAM), quantified as the sum of all the angles that the skeleton has in the volume normalized by the path length (rad/pixel) [16].

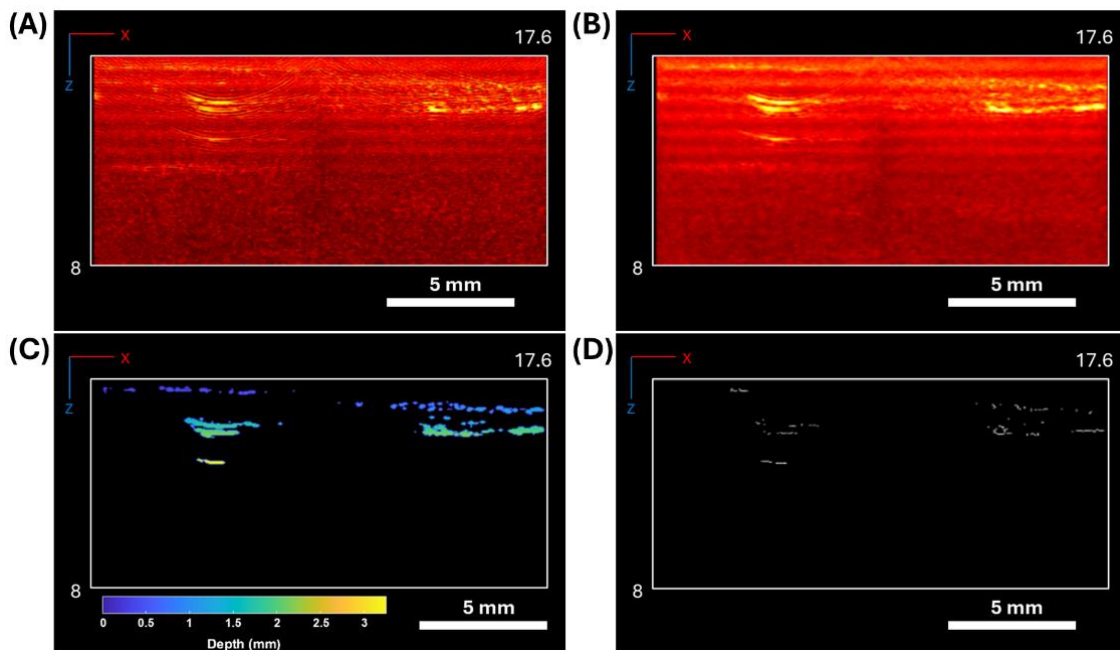


Figure 2. PA slices (X-Z) processing and skeleton extraction.

3. RESULTS

Here we present the preliminary results of employing a Kolo L38-22v CMUT high frequency probe coupled with the Verasonics Vantage 256 (High Frequency configuration) and demonstrate the feasibility of acquiring photoacoustic images of the skin and superficial vasculature at different body locations. Fig. 3 shows the 3D reconstruction of an example volume acquired on the wrist. Tab. 1 shows the average values of the quantitative parameters that were extracted from the skeletons.

Table 1. Average and standard deviation of the quantitative parameters across body locations.

Metric	NT	NB	VD	DM	ICM	SOAM
Average	2.80	49.20	0.0035	1.93	40.25	0.28
St. Dev.	1.92	39.73	0.0033	0.23	18.37	0.16

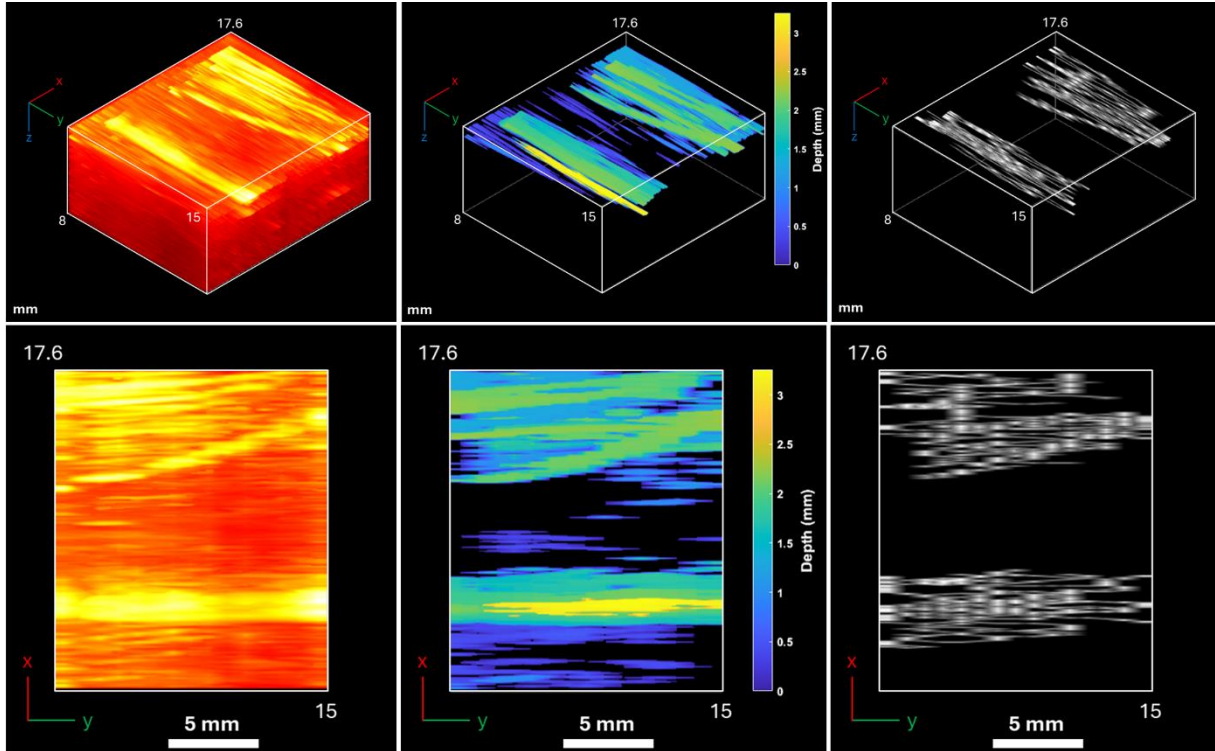


Figure 3. Example of normalized PA data, segmentation and skeleton of a volume acquired from a wrist, shown in a 3D view (first row) and top view (second row).

4. DISCUSSION AND CONCLUSION

As can be noted, while the proposed method effectively segments the photoacoustic image, it currently segments not only the blood vessels but also captures the top skin layer containing melanin, which influences the specificity of the segmentation. The poor signal quality presents an additional challenge, which in further studies will be enhanced by optimizing both the imaging setup and illumination as well as the signal and image processing methods that were employed. Although a definitive ground truth for full validation is unavailable, the approach remains valuable for comparative studies, as the quantitative parameters provide consistent metrics to evaluate relative differences between various conditions (e.g., healthy vs pathological). Overall, while the method demonstrates limitations in performance in its current form, it successfully establishes the feasibility of the approach employing a high frequency CMUT ultrasound transducer for photoacoustic imaging, providing a foundation for future improvements and optimization.

ACKNOWLEDGEMENTS

This study was carried out within the «Quantitative imaging of vascular dysregulation as a functional basis for autoimmune disorders and tumors (AI-VASCUES)» project – funded by European Union – Next Generation EU within the PRIN 2022

program (D.D. 104 - 02/02/2022 Ministero dell'Università e della Ricerca). This manuscript reflects only the authors' views and opinions and the Ministry cannot be considered responsible for them.

REFERENCES

- [1] L. Rey-Barroso, S. Pena-Gutierrez, C. Yanez, F. J. Burgos-Fernandez, M. Vilaseca, and S. Royo, "Optical Technologies for the Improvement of Skin Cancer Diagnosis: A Review," *Sensors (Basel)*, vol. 21, no. 1, Jan 2 2021, doi: 10.3390/s21010252.
- [2] M. Liu and W. Drexler, "Optical coherence tomography angiography and photoacoustic imaging in dermatology," *Photochemical & Photobiological Sciences*, 10.1039/C8PP00471D vol. 18, no. 5, pp. 945-962, 2019, doi: 10.1039/C8PP00471D.
- [3] J. Ahn, M. Kim, C. Kim, and W. Choi, "In vivo multi-scale clinical photoacoustic imaging for analysis of skin vasculature and pigmentation: a comparative review," *Advanced Imaging*, vol. 1, no. 3, 2024, doi: 10.3788/ai.2024.20005.
- [4] W. Choi, E. Y. Park, S. Jeon, and C. Kim, "Clinical photoacoustic imaging platforms," *Biomed Eng Lett*, vol. 8, no. 2, pp. 139-155, May 2018, doi: 10.1007/s13534-018-0062-7.
- [5] Y. Wang, Y. Zhan, M. Tiao, and J. Xia, "Review of methods to improve the performance of linear array-based photoacoustic tomography," *Journal of Innovative Optical Health Sciences*, vol. 13, no. 02, 2019, doi: 10.1142/s1793545820300037.
- [6] D. Ren, C. Li, J. Shi, and R. Chen, "A Review of High-Frequency Ultrasonic Transducers for Photoacoustic Imaging Applications," *IEEE Trans Ultrason Ferroelectr Freq Control*, vol. 69, no. 6, pp. 1848-1858, Jun 2022, doi: 10.1109/TUFFC.2021.3138158.
- [7] R. J. Zemp, R. Bitton, M. L. Li, K. K. Shung, G. Stoica, and L. V. Wang, "Photoacoustic imaging of the microvasculature with a high-frequency ultrasound array transducer," *J Biomed Opt*, vol. 12, no. 1, p. 010501, Jan-Feb 2007, doi: 10.1117/1.2709850.
- [8] J. Benavides-Lara, A. P. Siegel, M. M. Tsoukas, and K. Avnani, "High-frequency photoacoustic and ultrasound imaging for skin evaluation: Pilot study for the assessment of a chemical burn," *J Biophotonics*, vol. 17, no. 7, p. e202300460, Jul 2024, doi: 10.1002/jbio.202300460.
- [9] H. Zafar, A. Breathnach, H. M. Subhash, and M. J. Leahy, "Linear-array-based photoacoustic imaging of human microcirculation with a range of high frequency transducer probes," *J Biomed Opt*, vol. 20, no. 5, p. 051021, May 2015, doi: 10.1117/1.JBO.20.5.051021.
- [10] J. Chan, Z. Zheng, K. Bell, M. Le, P. H. Reza, and J. T. W. Yeow, "Photoacoustic Imaging with Capacitive Micromachined Ultrasound Transducers: Principles and Developments," *Sensors (Basel)*, vol. 19, no. 16, Aug 20 2019, doi: 10.3390/s19163617.
- [11] A. Caronti *et al.*, "Capacitive micromachined ultrasonic transducer (CMUT) arrays for medical imaging," *Microelectronics Journal*, vol. 37, no. 8, pp. 770-777, 2006, doi: 10.1016/j.mejo.2005.10.012.
- [12] M. Vallet *et al.*, "Quantitative comparison of PZT and CMUT probes for photoacoustic imaging: Experimental validation," *Photoacoustics*, vol. 8, pp. 48-58, Dec 2017, doi: 10.1016/j.pacs.2017.09.001.
- [13] S. Kulkarni, K. Dhingra, and S. Verma, "Applications of CMUT Technology in Medical Diagnostics: From Photoacoustic to Ultrasonic Imaging," *International Journal of Science and Research (IJSR)*, vol. 13, no. 6, pp. 1264-1269, 2024, doi: 10.21275/sr24619062609.
- [14] K. Kratkiewicz, R. Manwar, Y. Zhou, M. Mozaffarzadeh, and K. Avnani, "Technical considerations in the Verasonics research ultrasound platform for developing a photoacoustic imaging system," *Biomed Opt Express*, vol. 12, no. 2, pp. 1050-1084, Feb 1 2021, doi: 10.1364/BOE.415481.
- [15] M. Salvi and F. Molinari, "Multi-tissue and multi-scale approach for nuclei segmentation in H&E stained images," *Biomed Eng Online*, vol. 17, no. 1, p. 89, Jun 20 2018, doi: 10.1186/s12938-018-0518-0.
- [16] K. M. Meiburger, S. Y. Nam, E. Chung, L. J. Suggs, S. Y. Emelianov, and F. Molinari, "Skeletonization algorithm-based blood vessel quantification using in vivo 3D photoacoustic imaging," *Phys Med Biol*, vol. 61, no. 22, pp. 7994-8009, Nov 21 2016, doi: 10.1088/0031-9155/61/22/7994.